Research Journal of Information Technology

ISSN 1815-7432

Academic Journals Inc.

www.academicjournals.com

Research Journal of Information Technology 7 (1): 70-79, 2015
ISSN 1815-7432 / DOI: 10.3923/rjit.2015.70.79

Detection of Macular Drusen Based On Texture Descriptors

A. Rama Prasath and M.M. Ramya
Department of Computer Applications, Hindustan Institute of Technology and Science, Chennai, India

Corresponding Author: A. Rama Prasath, Department of Computer Applications, Hindustan Institute of Technology and Science, Chennai, India

ABSTRACT

Drusen located in the macula region which is responsible for the majority of useful photopic vision characterizes the Age-Related Macular Degeneration (ARMD). Variation in shape, size, degree of confluence and non-homogeneous texture of the drusen makes it a challenging task to build a classifier for macular drusen detection. To address this difficulty, an algorithm for drusen detection based on GLCM based textural features was proposed that is spatially adaptive to improve the robustness with increased accuracy while reducing the screening time. Localization of the Optic Disc (OD) and blood vessels using morphological operators aids in improving the accuracy of the classifier. Proposed algorithm detects macula region based on the location of the vascular arcades and the OD. The performance of the proposed system was evaluated by comparing the drusen detected output images with the hand-labelled ground-truth images graded by the experts. The Receiver Operating Characteristic (ROC) curve of the proposed system provides over 98.05% segmentation accuracy.

Key words: Macula, morphological operators, circular hough transform, texture descriptors

INTRODUCTION

The ARMD is the most common cause of irreversible vision loss in people over the age of 65 around the world (Checco and Corinto, 2006). This disease progressively degrades macula, a specific part of the eye that is responsible for fine and detailed central vision. The early stage of ARMD is drusen, accumulation of extra cellular materials anywhere in the retina (Prasath and Ramya, 2014a), yet the severity is more when the drusen is located in the macula region. This problem leads to consider the macula region as the area of interest which is located temporal to the optic disc and bounded by the temporal superior and inferior vascular arcades. Evaluation in a sequence of images taken during a long-term treatment, helps to understand the progression of the disease and the effectiveness of treatment. This evaluation is difficult to reproduce manually. Hence, there is a need for an automated system that will enable to formulate a standard which in turn will improve the follow up of ARMD.

An extensive literature survey was performed on methodologies that specifically focuses on drusen detection without human intervention. Histogram based methods were found to be efficient in classifying drusen (Rapantzikos *et al*., 2003). However, they tend to over segment at the border. Brandon and Hoover (2003) classified an image using multilevel approach, that detects more evident drusen but more number of false positives arises at pixel level classification. A square region of interest with 400×400 pixels in the macula region was alone considered from an image size of 1000×650 based on image gradient that classifies drusen (Mora *et al*., 2004).

Levenberg-Marquardt methodology is used to model each drusen spot with a maximum processing time and it fails to model drusen when optic disc in the image is not clearly visible (Moitinho *et al.*, 2008). Rapantzikos *et al.* (2003) used histogram based adaptive local thresholding technique to segment drusen spots but it fails to mark drusen that is located inside the bright background (Rapantzikos and Zervakis, 2001). The automated system for detecting drusen in the fundus image will positively improve the treatment of this abnormality.

In this study an algorithm is proposed to improve the efficiency of drusen detection based on non-homogenous textures in the macula region. These features helps the ophthalmologists to evaluate the progress of the disease.

MATERIALS AND METHODS

Pre-processing: Retinal images are acquired with a digital fundus camera that captures the illumination reflected from the retinal surface. Despite controlled conditions, several factors such as curved surface of retina, pupil dilation, unexpected movement, presence of cataract introduces severe distortions into the resulting image. These distortions are usually perceived as smooth intensity variations across the image and should be eliminated by enhancing the contrast and performing non-uniform illumination correction. The images captured by the fundus camera normally suffer with non-uniform illumination. Hence, drusen in one region is brighter than the other which makes the classification difficult. It can be compensated by performing homomorphic filtering by simultaneously compressing the brightness range. The fundus image often has a low contrast where the drusen resemble to smudge with the background and hence are not clear to the doctors. This may lead to wrong diagnosis. Hence, Contrast Limited Adaptive Histogram Equalization (CLAHE) (Lee *et al.*, 2008; Haller, 2011) is preferred for enhancing the contrast of the fundus image in proposed study where emphasis is more on local contrast than global contrast.

OD localization: The intensity of the OD region resembles with that of drusen, hence OD should be eliminated to reduce the number of false positive (Prasath and Ramya, 2014b). To efficiently detect OD, mathematical morphological operators are used (Amalopravam *et al.*, 2013). Dilation and erosion are two fundamental operators used as the basis for other operators such as open (ϕ) and close (ψ) etc. Let a function F^0: $R^2 \rightarrow R$ represent a 2-D signal and g: $B \rightarrow R^2$ be a structuring function representing the structural element with a compact support $B \subseteq R^2$. Dilation δ and erosion Σ of f^0 by g is defined as:

$$\delta g\left(f^0\right) = \max\left\{f^0\left(x - x', y - y'\right) + g\left(x', y'\right)\right\} \tag{1}$$

$$\Sigma g\left(f^0\right) = \min\left\{f^0\left(x + x', y + y'\right) - g\left(x', y'\right)\right\} \tag{2}$$

with x, y ϵf^0 and x,' yϵB.

A structuring element is used by selecting the size and shape of the neighbourhood construct. In an image to add the pixels to the boundaries, dilation is used and to remove the pixels from the boundary erosion is used. The shape and the size of the structuring element determines the number of pixels added or removed from the image.

Macula localization: Numerous hard drusen in the macula increase significantly the incidence of soft drusen and RPE abnormalities (Klein *et al*., 2007, 2002) which are, in turn, more likely to progress to the advanced stages of ARMD. Hence, Macula region is considered to be the Region of Interest (ROI) that comprises all relevant structure. This region is further responsible for color perception. The automatic ROI selection can be achieved with the following steps.

Retina localization: The retina localization assists to detect the macula region. The contribution of the retinal border to the photopic vision is very low, hence a combination of mathematical morphology and circular Hough transform is used to remove the borders of the retinal image. The OD detected retinal image remains binarized with global image threshold using Otsu's method. The Hough transform is described as a transformation of a point in the (x, y) plane to the parameter space (Gonzalez and Woods, 2000). The parameter space of a circle is given by the Eq. 3:

$$x\cos\theta+y\sin\theta = \rho \tag{3}$$

The point in the (x, y) space is now represented by a curve in (ρ, θ) space. The fovea is located between OD and the Macula region at a distance Dt = 2.5×D, where D defines the diameter of OD (Samanta *et al*., 2011). Then to segment the macula region circular Hough transform with a radius R = 5×D was used.

Blood vessel segmentation: In order to segment the superior and inferior vascular arcades along with the blood vessels morphological opening operator is applied on the retinal image I_1 to obtain I_2. Then morphological closing operator is used to remove the blood vessel present in the retinal image I_2 to obtain an image I_3. Then by applying a morphological top-hat transform (Samanta *et al*., 2011) that extracts small blood vessels, the image I_4, was obtain where the blood vessels alone will be segmented from the retinal image:

$$I_2 = \phi\ (I_1) \tag{4}$$

$$I_3 = \psi(I_2) \tag{5}$$

$$I_4 = (I_3\text{-}I_1) \tag{6}$$

Blood vessel labelling: Labelling the blood vessels helps to detect the superior and inferior vascular arcades. Labelling the binary image B can be written as g: B→N where g(x,y) is described as:

$$g(x,y) = \begin{cases} F_b \text{if } P(x,y) = F_b \\ l_k \text{if } p(x,y) \in C_k \end{cases} \tag{7}$$

where, k defines the total number of connected components, l_k be a new label, C_k be the connected component, each pixels $\rho \epsilon B$ corresponds to the background F_b or foreground F_f, respectively. It computes by combining the pixels which are symmetric about its center element (Walczyk *et al*.,

2010). The number of pixels that share a same label helps to calculate the area of each blood vessel. The blood vessels with same label D_{max} is described as:

$$D_{max} = \max\left\{\sum_{r=1}^{k} g_{x,y} == r \mid x = 1..m, y = 1..n\right\} \tag{8}$$

where m, n corresponds to the total number of rows and columns of the labelled image, respectively.

Texture feature extraction: Gray-Level Co-occurrence Matrix (GLCM) is a statistical method aimed at examining the gray level transition between two pixels (Zulpe and Pawar, 2012). It characterizes the texture of the image by calculating how often pairs of pixels with specific value and in a specified spatial association ascend in an image, by creating a GLCM where the statistical measure can be extracted from the matrix. This method creates a co-occurrence matrix by calculating how often a pixel with a particular gray level intensity value i occurs in a specific spatial relationship to a pixel with a value j with a certain distance d and orientation θ. The number of rows and columns of a GLCM matrix depends on the graylevels G in the texture of an image. The relative frequency of a matrix $P(i, j \mid \Delta x, \Delta y)$ is separated by a pixel distance $(\Delta x, \Delta y)$. $P(i, j \mid d, \theta)$ is a matrix element which contains the second order probability values for gray level i and j at distance d and orientation θ:

$$p_x(i) = \sum_{j=0}^{G-1} p(i, j)$$

and:

$$p_y(j) = \sum_{i=0}^{G-1} p(i, j)$$

are the i-th and j-th entry obtained by summing the rows of P(i,j).

Various features can be extracted from the GLCM, μ the mean value of P, σ is the standard deviation of P. To calculate the different textural features contained in the co-occurrence matrices Haralick *et al.* (1973) proposed various statistical measures. In order to classify drusen from the background three texture features have been used to train the classifier. The features used for classification are as follows:

- **Autocorrelation:** It is used to compute the gray tone linear dependencies of the drusen in the retinal image:

$$AUTOC = \sum_{i=0}^{G-1}\sum_{j=0}^{G-1} \frac{\{i \times j\} \times p(i, j) - \{\mu_x \times \mu_y\}}{\sigma_x \times \sigma_y} \tag{9}$$

The value ranges between -1 to 1, -1 infers maximally uncorrelated and 1 implies maximally correlated.

- **Sum average:** It is used to measure the average skewness for each image by calculating the section-based skewness of the image:

$$\text{Aver} = \sum_{i=0}^{2G-2} i p_{x+y}(i) \tag{10}$$

- **Sum variance:** It is a measure of heterogeneity and its variance increases when the gray level values differ from their mean:

$$\text{SVAR} \sum_{i=0}^{2G-2} (i - f_s)^2 \, p_{x+y}(i) \tag{11}$$

Using these second order textural features the drusen regions that differs from the macula region will be identified.

RESULTS AND DISCUSSION

The images used for the proposed work were collected from Aravind eye hospital-Madurai and publicly available databases such as STARE and DRIVE. The proposed method is implemented in MATLAB. To reduce the processing time the RGB channel with maximum contrast which permits better classification of the drusen from the background was passed as an input for further processing.

Figure 1 shows the retinal image and its highest graininess channel. The selected channel was pre-processed with CLAHE and homomorphic filtering to enhance the contrast and correct the illumination. The OD was localized as described in our previous work (Prasath and Ramya, 2014a). The intensity based retinal image was binarized by Otsu threshold. The small dark regions with

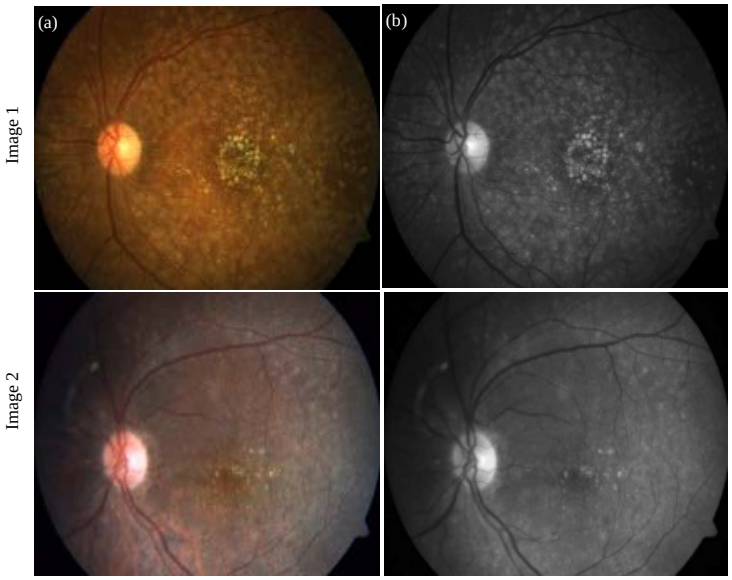

Fig. 1(a-b): Input retinal image and its highest graininess channel, (a) Fundus color image and (b) Input color channel

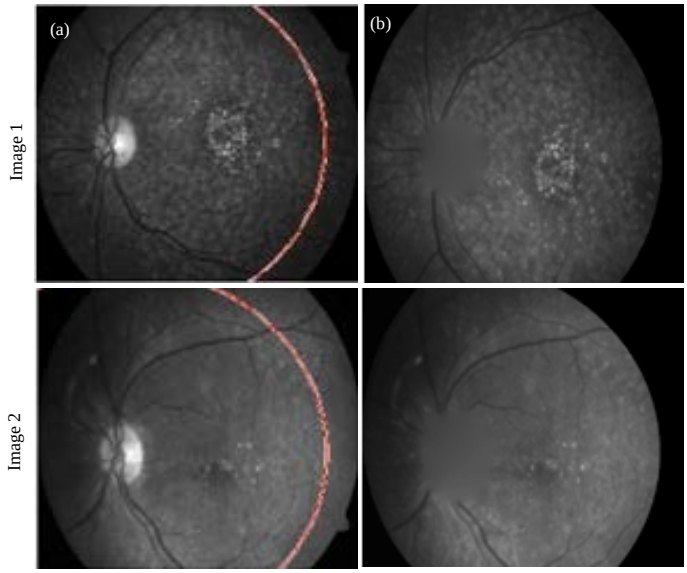

Fig. 2(a-b): Retinal (a) Borders marked and (b) OD and Border eliminated image

Table 1: Threshold for textural features

Textural features	Drusen region
Autocorrelation	35.96±12.55
Sum average	11.76±2.100
Sum variance	133.82±53.60

intensity lesser than the Otsu threshold can be removed by performing morphological dilation with a disk shape structuring element. The diameter of the OD was 77.9 and 74.03 for Image 1 and Image 2, respectively. The localized retina leads to the determination of the size of the retina. Figure 2 shows the retinal image where the borders have been properly removed.

As stated in retina localization, the circular Hough transform with a radius 389.53 and 370.18 for Images 1 and 2, respectively, were used to remove the borders leading to effective segmentation of drusen. The blood vessels can be effectively detected using morphological top-hat transform. By using connected component analysis the superior and the inferior arcades can be effectively segmented.

Figure 3 shows the segmented blood vessels and the superior and inferior arcades of the retina. A circle fitting is done in x, y plane with the coordinates of the blood vessel. The region that lies within the circle represents the macula and is considered for further processing. The ROI is extracted by eliminating the regions posterior to the retinal vascular arcades which comprises all relevant structures, hence the overall amount of data is reduced in each direction which accelerates subsequent computations. Figure 4 shows the segmented macula region.

Figure 5 shows the drusen in the macula region.

The drusen located in the macula region are segmented based on the common textural features from GLCM. The threshold for the textural features are listed in Table 1.

Sensitivity and specificity are used as a measure to evaluate the accuracy of the proposed system. The FAR and FRR obtained in the proposed study are listed in Table 2.

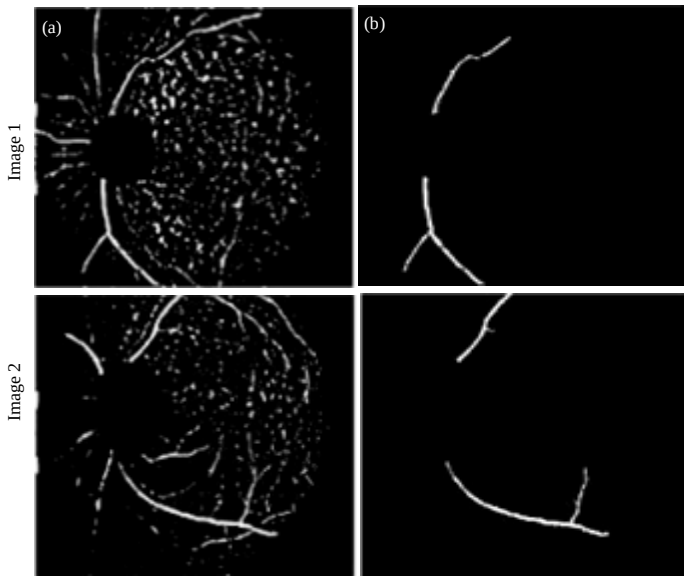

Fig. 3(a-b): (a) Blood vessels and (b) Retinal vascular arcades segmented image

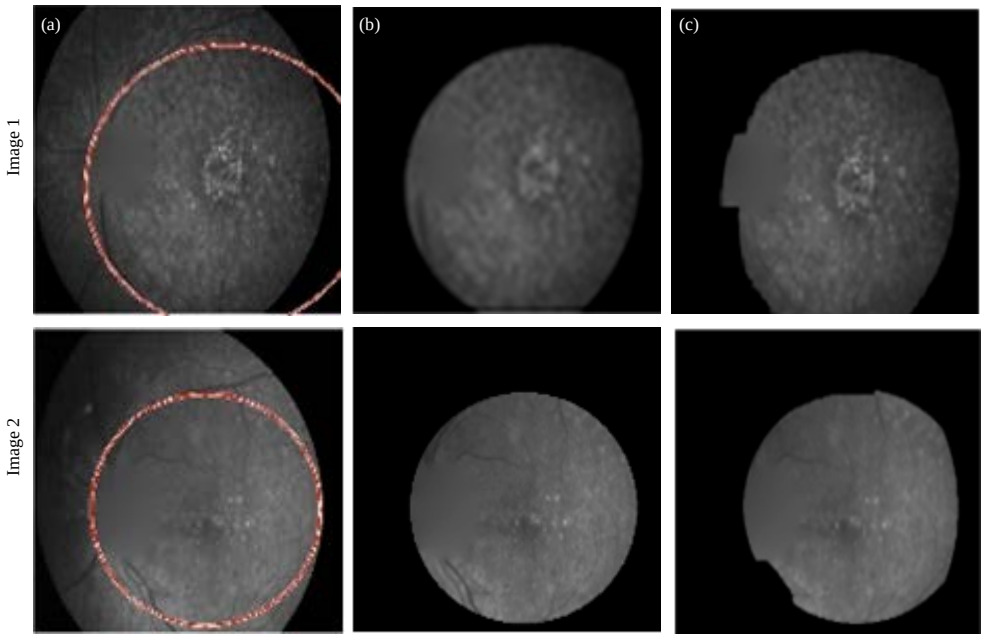

Fig. 4(a-c): Macula ROI region segmented image, (a) Macula region morked, (b) Segmented macula region and (c) ROI segmented region

One hundred and twenty samples were considered for individual drusen types to compute FAR and FRR. Table 2 shows the results obtained in classification of drusen under each grade. It was observed from the table that 120 samples were exactly identified as large drusen with no false positives resulting in 100% accuracy. In case of medium drusen, the proposed system correctly

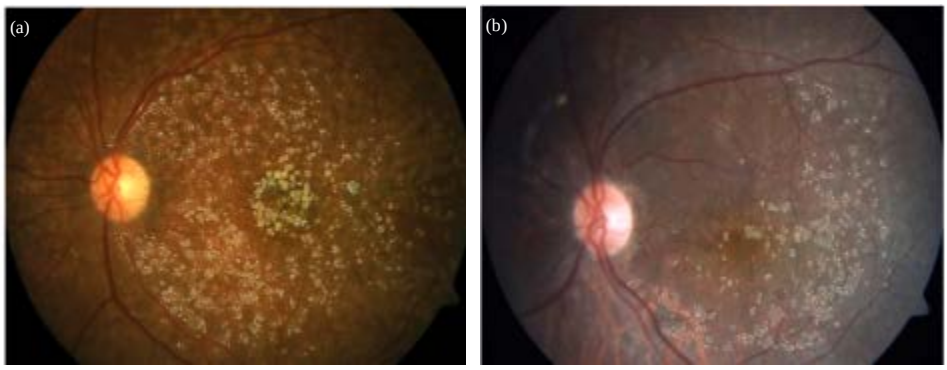

Fig. 5(a-b): Drusen detected image, (a) Image 1 and (b) Image 2

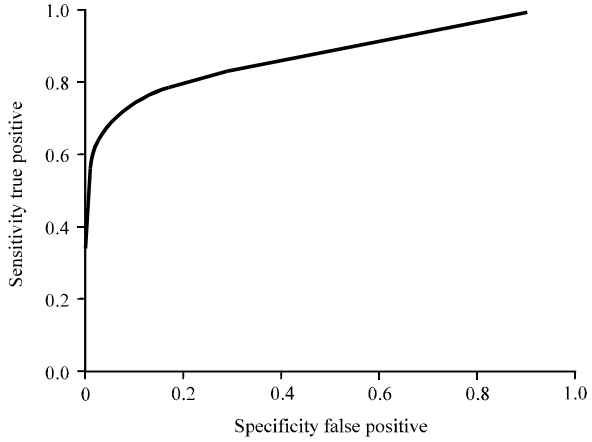

Fig. 6: ROC curve of an automated drusen detection algorithm

Table 2: Performance evaluation

Drusen type	FRR (%)	FAR (%)
Large drusen (>125 μm)	0.0	0.0
Medium drusen (63-125 μm)	1.6	0.83
Small drusen (<63 μm)	4.1	5.8

classified 118 samples and misclassified 2 sample regions (1 background sample and 1 small drusen region marked as medium drusen). Similarly 115 samples have been correctly classified to be small drusen and 5 samples are misclassified to be small drusen. There is an increase in the FAR of small drusen. This is because the background samples that has a minimum texture variation are misclassified as small drusens. The proposed system was able to identify 353 drusens out of 360 drusens yielded 98.05% accuracy.

The Receiver Operating Characteristic (ROC) curve of automated drusen detection was used to distinguish the relationship between sensitivity and specificity. The performance of the proposed system will be better when the ROC curve approaches closer to the top left corner.

The ROC curve reflects that the proposed system agrees with the ground truth detection. Figure 6 shows the ROC curve of automated drusen detection algorithm.

CONCLUSION

In this study, a novel medical decision support system has been developed to automatically detect drusen from the retinal imagethat will improve the quality of the follow up of ARMD. The proposed algorithm involves pre-processing which is responsible for non-uniform illumination correction and contrast enhancement that are the common problems found in retinal images. The image was subjected to morphological top-hat transform to detect the blood vessels and the selected features are properly labelled to segment the macula region. This study presents a new method to quantitatively measure drusen texture features based on GLCM. The algorithm was validated with 40 images graded by medical experts. In our work, the performance was assessed using ROC curve which shows 98.5% of accuracy in quantifying the relevant drusen. Future work will be focused towards reducing the processing time.

ACKNOWLEDGMENT

The authors thank the management of Hindustan Institute of Technology and Science for rendering their continuous support, encouragement and cooperation throughout the progress of the work. We would also like to thank Dr. Kim and Dr. Renu of Aravind Eye Hospital, Madurai for providing dataset.

REFERENCES

Amalopravam, G., T.H. Naik and J. Kumari, 2013. Transformation of digital images using morphological operations. Int. J. Comput. Sci. Inform. Technol., 1: 22-28.

Brandon, L. and A. Hoover, 2003. Drusen detection in a retinal image using multi-level analysis. Proceedings of the 6th International Conference on Medical Image Computing and Computer-Assisted Intervention, November 15-18, 2003, Montreal, Canada, pp: 618-625.

Checco, P. and F. Corinto, 2006. CNN-based algorithm for drusen identification. Proceedings of the IEEE International Symposium on Circuits and Systems, May 21-24, 2006, Island of Kos, Greece, pp: 2181-2184.

Gonzalez, R. and R. Woods, 2000. Digital Image Processing. 2nd Edn., Prentice Hall, New Jersey, USA.

Haller, E.A., 2011. Adaptive histogram equalization in GIS. Ann. Univ. Craiova Math. Comput. Sci. Ser., 38: 100-104.

Haralick, R.M., K. Shanmugam and I. Dinstein, 1973. Textural features for image classification. IEEE Trans. Syst. Man Cybern., SMC-3: 610-621.

Klein, R., B.E.K. Klein, S.C. Tomany, S.M. Meuer and G.H. Huang, 2002. Ten-year incidence and progression of age-related maculopathy: The Beaver Dam eye study. Ophthalmology, 109: 1767-1779.

Klein, R., B.E. Klein, M.D. Knudtson, S.M. Meuer, M. Swift and R.E. Gangnon, 2007. Fifteen-year cumulative incidence of age-related macular degeneration: The Beaver Dam eye study. Ophthalmology, 114: 253-262.

Lee, M., A.F. Laine and T.R. Smith, 2008. Learning non-homogenous textures and the unlearning problem with application to drusen detection in retinal images. Proceedings of the 5th IEEE International Symposium on Biomedical Imaging: From Nano to Macro, May 14-17, 2008, Paris, France, pp: 1215-1218.

Moitinho, F., R. Mora, P. Vieira and J. Fonseca, 2008. A drusen volume quantification method based on a segmentation algorithm. Proceedings of the 1st ECCOMAS Thematic Conference on Computational Vision and Medical Image Processing, October 17-19, 2007, Porto, Portugal, pp: 957-962.

Mora, A., P. Vieira and J. Fonseca, 2004. Drusen deposits on retina images: Detection and modelling. Proceedings of the 2nd International Conference on Advances in Medical Signal and Information Processing, September 5-8, 2004, Malta, pp: 241-248.

Prasath, A.R. and M.M. Ramya, 2014a. Automatic detection and elimination of an optic disc for improving drusen detection accuracy. Proceedings of the 5th International Conference on Signal and Image Processing, January 8-10, 2014, Jeju Island, pp: 117-120.

Prasath, R.A. and M.M. Ramya, 2014b. Automated drusen grading system in fundus image using fuzzy C-means clustering. Int. J. Eng. Technol., 6: 833-841.

Rapantzikos, K. and M. Zervakis, 2001. Nonlinear enhancement and segmentation algorithm for the detection of Age-related Macular Degeneration (AMD) in human eye's retina. Proceedings of the International Conference on Image Processing, Volume 3, October 7-10, 2001, Thessaloniki, Greece, pp: 1055-1058.

Rapantzikos, K., M. Zervakis and K. Balas, 2003. Detection and segmentation of drusen deposits on human retina: Potential in the diagnosis of age-related macular degeneration. Med. Image Anal., 7: 95-108.

Samanta, S., S.K. Saha and B. Chanda, 2011. A simple and fast algorithm to detect the fovea region in fundus retinal image. Proceedings of the 2nd International Conference on Emerging Applications of Information Technology, February 19-20, 2011, Kolkata, India, pp: 206-209.

Walczyk, R., A. Armitage and T.D. Binnie, 2010. Comparative study on connected component labeling algorithms for embedded video processing systems. Proceedings of the World congress in Computer Science Computer Engineering and Applied Computing, July 12-15, 2010, Las Vegas, NV., USA., pp: 853-859.

Zulpe, N. and V. Pawar, 2012. GLCM textural features for brain tumor classification. Int. J. Comput. Sci., 9: 354-359.